

Bromination and Gas Permeability of Poly(1-trimethylsilyl-1-propyne) Membrane

K. NAGAI, A. HIGUCHI, and T. NAKAGAWA*

Department of Industrial Chemistry, Meiji University, Higashi-mita, Tama-ku, Kawasaki 214, Japan

SYNOPSIS

The bromination of poly(1-trimethylsilyl-1-propyne) (PMSP) was carried out by immersing a PMSP membrane in bromine water at 25°C. The bromine mainly reacted at the carbon-carbon double bonds in the backbone chain, and carbon-carbon single bonds were produced, which was determined from the infrared (IR) and ultraviolet (UV)-visible analyses. The glass transition temperature of the PMSP is above 350°C, but a new endothermic peak appeared between 50 and 80°C in the differential scanning calorimetry (DSC) curves of all brominated PMSPs. The permeability for 12 gases in the PMSP membrane and its brominated membranes was investigated between 30 and 90°C below 1 atm. With increasing bromine content in the membrane, the permeability coefficient for all gases decreased together with the diffusion coefficient, and the ideal separation factor for the industrially important gas pairs increased at 30°C. A distinct change in slopes at near the endothermic temperature determined by the DSC analysis was observed in Arrhenius plots of the permeability coefficients in all brominated PMSP membranes. © 1994 John Wiley & Sons, Inc.

INTRODUCTION

The industrialization of polymeric membrane processes has grown rapidly since the 1970s because of an increase in our commercial needs. The development of new membrane materials has been expected to produce both high permeability and high selectivity. Masuda's group reported the excellent permeability for gases in a poly(1-trimethylsilyl-1-propyne) (PMSP) membrane in 1983.¹ Many groups have reported various modifications and fundamental studies of this polymer.¹⁻²² However, the PMSP membrane's biggest problem is the deterioration of its high permeability with time or thermal hysteresis. This suggests the physical aging of its large excess free volume in the unrelaxed domains of this glassy polymer.

This study was completed as part of the solution of this problem through chemical modifications. The authors thought that halogenation of the PMSP was useful for the reaction with groups that would pre-

vent physical aging, in addition to other functional groups, e.g., various groups with gas affinities and hydrophilic groups. A brominated PMSP (Br-PMSP) membrane, itself, showed unusual gas transport behavior. In this study, the bromination of the PMSP membrane and its permeability were investigated in detail.

There are several studies about the halogenation of PMSP, i.e., surface treatment with fluorine gas⁷ and bromination with *N*-bromosuccinimide in a carbon tetrachloride solution.⁸ In the latter case, the bromination occurred at the allyl-type methyl group in the PMSP while the carbon-carbon double bond in the backbone chain did not react because of the steric hindrance of the large trimethylsilyl groups. There is a study that reports that the reaction of the PMSP with Br₂ did not occur.⁵

EXPERIMENTAL

Preparation of PMSP Membrane

PMSP was synthesized under dry nitrogen using TaCl₅ in toluene at 80°C for 24 h; [1-trimethylsilyl-1-propyne] = 0.3M, [TaCl₅] = 0.02M.^{23,24} The prod-

* To whom correspondence should be addressed.

uct was precipitated from a large amount of methanol. The precipitate was filtered and dried under vacuum. The yield was 80%. The weight- (M_w) and number- (M_n) average molecular weights of the product were 540,000 and 220,000, respectively. These values were determined using gel permeation chromatography. The polydispersity ratio (M_w/M_n) was 2.4. The chemical structure was determined by FTIR and $^1\text{H-NMR}$ analyses and identified as PMSP.

The homogeneous PMSP membranes with between 50 and 500 μm thicknesses were prepared by the casting method. The synthesized PMSP was dissolved in toluene; then the solution was cast onto a glass plate and dried under vacuum. All membranes were immersed in methanol to keep the membranes fresh.

Bromination of PMSP Membrane

Bromination was carried out by immersing the PMSP membrane in bromine water containing 1–2% bromine at 25°C. The membrane was fixed to a depth of 1.0 cm below the liquid surface using some glass hooks. The degree of bromination was controlled by the reaction time. The unreacted bromine in the membrane was completely washed out with water, and the membrane was dried under vacuum for 24 h. Using the flask combustion method, the combined bromine content of the membrane was determined.

Characterization Analyses

The FTIR spectra were recorded on a FTIR Perkin-Elmer 1800 by the KBr method and the total internal reflection (ATR) method at a resolution of 4 cm^{-1} . A KRS-5 crystal was used and the incident angle to the crystal was 45°. Ultraviolet (UV)–visible absorption spectra were obtained at 25°C in cyclohexane using a Hitachi Model 200-20. Differential scanning calorimetry (DSC) was determined using a Perkin-Elmer DSC 7 at a heating rate and a cooling rate of 20°C/min. Gel permeation chromatography was done using a Tohsoh HLC-8020. M_w and M_n were determined on the basis of a polystyrene calibration. Wide-angle x-ray diffraction spectroscopy was done using a Shimadzu XD-3A (Cu-K α). Bromine content was obtained by the flask combustion method using a Hamada FHO-1-A.

Measurement of Gas Permeability

The gas permeability was determined by the vacuum-pressure method.²⁵ The transport theory and

calculation of the permeability, diffusion, and solubility coefficients were done according to the general method.^{25–27}

The experimental method used in this study was an adaptation of the high-vacuum gas transmission technique using an MKS Baratron Model 310BHS-100SP pressure transducer below 1 atm upstream pressure between 30 and 90°C. The pure gases, i.e., H_2 , He, D_2 , O_2 , N_2 , Ar, CO_2 , CH_4 , C_2H_4 , C_2H_6 , C_3H_6 , and C_3H_8 , were obtained from Showa Denko Co., Ltd. and Takachiho Co., Ltd., and used without further purification.

The permeability coefficient (P) was calculated from the slope of the time–pressure curves in the steady state. The diffusion coefficient (D) was determined using the time lag method;

$$D = 6\theta/L^2 \quad (1)$$

where θ is the time lag and L is the thickness. The solubility coefficient (S) was given by

$$S = P/D \quad (2)$$

The apparent activation energies of permeation (E_p), diffusion (E_D), and the enthalpy of solution (ΔH_s) were given by the following equations:

$$P = P_0 \exp(-E_p/RT) \quad (3)$$

$$D = D_0 \exp(-E_D/RT) \quad (4)$$

$$S = S_0 \exp(-\Delta H_s/RT) \quad (5)$$

$$\Delta H_s = E_p - E_D \quad (6)$$

where P_0 , D_0 , and S_0 are the preexponential factors, R is the gas constant, and T is the absolute temperature.

RESULTS AND DISCUSSION

Characterization of Br-PMSP

A slight yellow transparent membrane was formed from the synthesized PMSP. As bromination of the PMSP membrane proceeded, the transparency gradually disappeared and the color changed to a bright yellow.

Figure 1 shows the FTIR-ATR spectra of the PMSP and Br-PMSP (Br: 6.8 wt %) membranes. The FTIR spectra of the total Br-PMSP membrane, i.e., the surface and bulk, were also measured by the KBr method and had almost the same spectra mea-

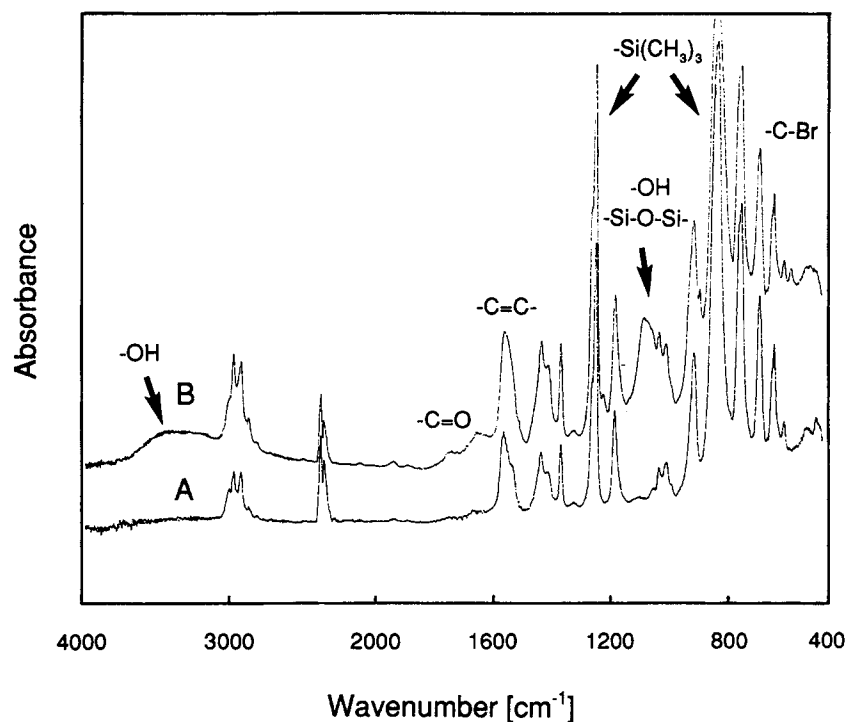


Figure 1 FTIR-ATR spectra of (a) the PMSP and (b) brominated PMSP (Br: 6.8 wt %) membranes.

sured by the ATR method. In this study, the bromine content has been described using total bromine content of the surface and bulk. New bands appeared after the bromination. There are the broad band between 4000 and 3200 cm^{-1} , two bands between 1800 and 1600 cm^{-1} , some bands near 1100 cm^{-1} , and the band near 720 cm^{-1} in the Br-PMSP membrane. These bands are due to the hydroxyl (OH), carbonyl (C=O), OH, and/or siloxane bond (Si—O—Si) and carbon-bromine (C—Br) groups, respectively. The top wavenumber of the band assigned to the carbon-carbon double bond (C=C) shifted by 17 cm^{-1} from 1561 to 1544 cm^{-1} and the absorbance weakened in comparison with the PMSP membrane. This result indicates that the C=C bond acted as one of the reaction sites. However, there is a study that reports the C=C bonds in the PMSP backbone chain could not react with Br_2 .⁵ Therefore, the behavior of the C=C bonds was analyzed in detail.

If the Br_2 reacts with the C=C bond and the —CBr—CBr— bond is produced, the C=C unit/Br atom ratio is 0.5. Figure 2 shows the relationship between Br concentration and C=C unit concentration estimated from the IR and UV-visible analyses. The densities of the Br-PMSP membranes were considered for calculating the Br concentration. The decrease in the true absorbances of the C=C

bond in the IR spectra was determined by quantitative infrared analysis using the peak height method. The band at 1246 cm^{-1} , which is assigned to the CH_3 symmetric deformation of the $\text{Si}(\text{CH}_3)_3$ group, was used as a reference. The C=C concentration of the PMSP was calculated using the molecular formula and the density. In the case of UV-visible analysis, the decrease in the C=C unit was

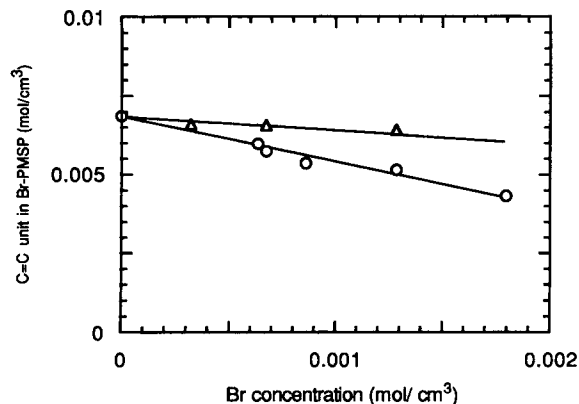


Figure 2 Relationship between bromine concentration and carbon-carbon double bond unit concentration estimated by (○) IR and (△) UV-visible analyses of the brominated PMSP membranes.

evaluated by the decrease in ϵ max at each λ max. The λ max of the PMSP was 221 (nm) and those of the Br-PMSPs used in this work were between 221 and 220 (nm). Both relations in Figure 2 show linearity. The slopes given by the IR and UV-visible analyses are -1.42 and -0.45 , respectively. Since the OH and C=O groups were observed in Figure 1, this result suggests that some C—Br bonds successively reacted with water and oxygen in air and changed to the —OH and C=O groups. Therefore, the slope's value given by the IR analysis was smaller than that given by the UV-visible analysis.

Most polymers show an endothermic peak, which denotes their glass transition temperature (T_g) between -130 and 300°C in their DSC curves.²⁸ The T_g of PMSP is known to be above 300°C .^{4,23,24} Figure 3 shows the DSC curves of the fresh PMSP and Br-PMSP membranes. The bromine content in the Br-PMSP was 18.4 wt % and the membrane stored in air at room temperature for 1 month was used as a sample. The heating-cooling cycle was done twice between 20 and 350°C at a scanning (both a heating and a cooling) rate of $20^\circ\text{C}/\text{min}$. At 350°C , the temperature was not held and was instantly reduced. Although no thermic change was observed in the PMSP membrane, a new endothermic transition point near 60°C appeared reversibly in the heating regions [see Fig. 3(b) and (d)] of the Br-PMSP DSC measurement. There is the exothermic peak near 250°C in the first heating, but this peak disappeared

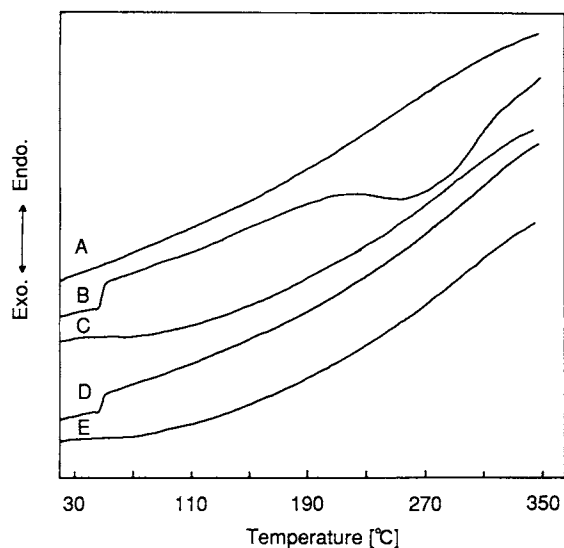


Figure 3 DSC curves of (a) the fresh PMSP membrane in the heating region and the brominated PMSP (Br: 18.4 wt %) membrane in the (b) first heating, (c) first cooling, (d) second heating, and (e) second cooling regions between 20 and 350°C .

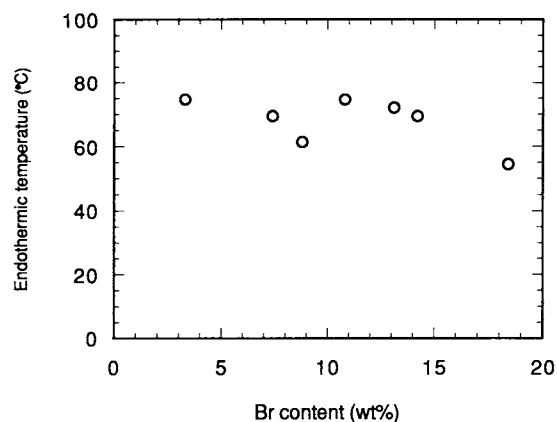


Figure 4 Relationship between bromine content and endothermic temperature in the DSC curves of the brominated PMSP membranes stored in air between the first day and 1 month.

in the second heating. No peaks were observed in the cooling regions. Figure 4 shows the relationship between bromine content and endothermic temperature in the first heating DSC curves of the Br-PMSP membranes stored in air at room temperature between the first day and 1 month. Their thicknesses were about $200\ \mu\text{m}$. In spite of the bromine content, endothermic transition points appeared between 50 and 80°C . Even if the bromine content was only 3 wt %, the peak was clearly observed. This suggests that the transition is attributable to the movement change (rotation) in the C—C bonds produced by the bromination. This phenomenon was probably due to those fundamental structures, i.e., the produced C—C bonds, therefore, the endothermic transition temperature was constant.

The band at $1100\ \text{cm}^{-1}$ appeared in Figure 1(b), and we have mentioned that this was due to the OH and/or Si—O—Si groups. If this bond is due to the Si—O—Si bonds, the crosslinking sections would also be formed, and then the gel fraction would be produced. The solubilities of the PMSP and Br-PMSP membranes at 25°C were investigated as shown in Table I. The bromine content in the Br-PMSP was 6.5 wt % and the thickness was $160\ \mu\text{m}$. The solubility parameter of the PMSP is $7.7\ (\text{cal}/\text{cm}^3)^{0.5}$, which is calculated according to Fedors constant,²⁹ but that of the Br-PMSP was not determined because of the mixed structures. However, since the bromine atoms were connected, the value of the Br-PMSP suggests to be larger than that of the PMSP. The Br-PMSP could dissolve in many solvents, therefore, it was assumed that there were few crosslinking sections. In comparison with the PMSP, the Br-PMSP showed a different solubility,

Table I. Solubility of the PMSP and Brominated PMSP (Br-PMSP, 6.5 wt %) Membranes at 25°C

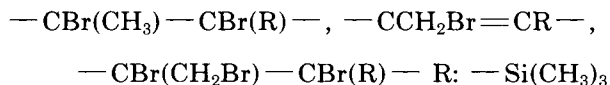
Solvent	δ^a	PMSP	Br-PMSP
Hexane	7.3	S	I
Diethyl ether	7.4	I	I
Cyclohexane	8.2	S	S
Carbon tetrachloride	8.6	S	S
Toluene	8.9	S	S
Tetrahydrofuran	9.1	S	S
Benzene	9.2	S	S
Chloroform	9.3	S	S
Dichloromethane	9.7	I	S
Ethylene dichloride	9.8	I	I
Acetone	9.9	I	I
1,4-Dioxane	10.0	I	I
Pyridine	10.7	I	I
Dimethyl acetamide	10.8	I	I
N-Methyl pyrrolidone	11.3	I	I
Dimethyl sulfoxide	12.0	I	I
N,N-Dimethyl formamide	12.1	I	I
Ethanol	12.7	I	I
Methanol	14.5	I	I
Water	23.4	I	I

^a Solubility parameter, (cal/cm³)^{0.5}, Ref. 29. (S) Soluble, (I) insoluble.

i.e., the Br-PMSP was soluble in dichloromethane but insoluble in hexane. The Br-PMSP membrane was easily reacted with some functional groups, e.g., an amino compound. The reactivity of the Br-PMSP membranes and their permeability will be reported in further publications.

After bromination, the viscosity of the Br-PMSP decreased. This suggests that the decomposition also occurred on the backbone chain.

From the results already presented, the products are thought to have the following structures:



Furthermore, from the effects of water and oxygen in air, some C—Br bonds would change the C=O and OH groups.

Thickness Dependence of Bromination

In order to analyze bromine content from the surface to the center, the Br-PMSP membranes were sliced from the surface to the center, and the bromine content of each slice was measured. Their values were

almost constant in spite of the depths of the measured slice. Total bromine content, i.e., the surface + bulk, approached the maximal value of about 20 wt % in spite of the thickness. The bromination occurred not only on the surface but also in the bulk between 50 and 500 μm of thickness when the total bromine content was above 8 wt %. However, below 8 wt % in which the reaction time was below 10 min, the thicker membrane had a thickness dependence. Above a 250 μm thickness, the bromine content decreased as one approached the center. In the case below 250 μm , there was no thickness dependence.

It is well known that the diffusibility for penetrants in a polymer is proportional to their molecular diameters.^{26,27} The diffusion coefficient (D) for some gases, e.g., C_3H_8 , CCl_2F_2 , and SF_6 in the PMSP membrane was about 10^{-6} (cm²/s). The diffusibility for Br_2 in the membrane suggests the same order. According to the time lag method, when D is 10^{-6} (cm²/s) and L is 250 μm (the diffusion would occur from both sides of the membrane having a 500 μm thickness), θ is below 2 min. The solubility coefficient (S) for chlorine gas in polyethylene film is larger than those for the light gases, e.g., CO_2 , O_2 , and N_2 , therefore, the permeability coefficient is also larger than those for the light gases.³⁰ This suggests that S for Br_2 in the PMSP membrane is larger than those for other gases. According to the solution-diffusion theory, the permeability coefficient for Br_2 would have a large value in comparison with other gases.

There are the kinetic studies of olefin bromination.³¹⁻³⁴ Most studies are discussed using the second- and third-order rate constants. The decrease in the C=C unit in the Br-PMSP membrane, which was evaluated by the IR analysis shown in Figure 2, was proportional to the increase in the bromine content with reaction time. The conversion of the C=C unit was determined as shown in Figure 5. The bromination up to 10 min, which had a thickness dependence, showed a first-order reaction. If a large amount of Br_2 was used in comparison with the PMSP, then the rate constant is given by

$$\ln[a/(a-x)] = k_1 t \quad (7)$$

where a is the initial C=C concentration, x is the concentration at time t , and k_1 is the rate constant of 2.32×10^{-4} (s⁻¹).

From the results presented above, it is clear that the bromination of the PMSP membrane can occur not only on the surface but also in the bulk. In comparison to the diffusion of bromine atoms in the

membrane, the reaction of bromine with the PMSP was the rate-determining step.

Gas Permeability of Br-PMSP

When the bromine content in the polymer was over 15 wt %, the membrane was brittle and easily cracked. Therefore, the membranes below 15 wt % bromine content were used for all gas permeation measurements.

The permeability coefficients for 12 gases and ideal separation factors for the industrial important gas pairs of the Br-PMSP membranes at 30°C are summarized in Table II. The measurements were carried out between 12 and 48 h after placing the membrane in the permeation apparatus. The thicknesses of the PMSP and Br-PMSP membranes were about 400 and 200 μm , respectively. The permeability coefficients for eight gases, i.e., H_2 , He, D_2 , O_2 , N_2 , Ar, CO_2 , and CH_4 , were constant below 1 atm, but for the other gases, i.e., C_2H_4 , C_2H_6 , C_3H_6 , and C_3H_8 , there was a pressure dependence. With increasing the pressure, the permeability coefficients for C_2H_4 , C_2H_6 , C_3H_6 , and C_3H_8 decreased. These values at 20 cm Hg are listed in Table II. There was little thickness dependence on the permeability coefficient. Most permeability coefficients of the Br-PMSP membranes for contents over 15 wt % bromine were 10^{-7} [cm^3 (STP) $\text{cm}/\text{cm}^2 \times \text{s} \times \text{cm Hg}$]. With increasing bromine content, all permeability coefficients decreased and all ideal separation factors increased. In the case of the separation for the H_2/CH_4 and $\text{C}_2\text{H}_4/\text{C}_2\text{H}_6$ pairs, the PMSP membrane has CH_4 and C_2H_6 selectivity, however, a selectivity change was observed after bromination. The separation of H_2/D_2 was also observed.

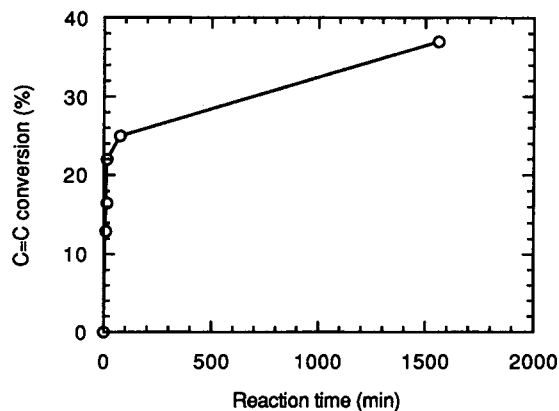


Figure 5 Time conversion ratio of carbon-carbon double bond unit concentration determined by IR spectra of the brominated PMSP membranes.

Table II. Comparison of Permeability Coefficients^a and Ideal Separation Factors of the Brominated PMSP Membranes at 30°C

Gas	Bromine Content (wt %)			
	0	3.3	10.8	13.1
H_2	13.9	7.36	2.72	2.16
D_2	9.71	—	2.22	1.73
He	5.25	—	1.29	1.04
O_2	7.85	3.75	1.38	1.01
N_2	5.51	2.06	0.66	0.45
Ar	6.97	—	1.18	0.84
CO_2	28.1	16.3	6.66	4.95
CH_4	14.5	5.14	1.65	1.08
C_2H_4	24.2	—	3.66	2.28
C_2H_6	27.4	—	3.60	2.17
C_3H_6	56.5	—	8.14	4.78
C_3H_8	34.0	—	3.78	2.04
O_2/N_2	1.42	1.82	2.10	2.26
H_2/N_2	2.52	3.57	4.15	4.84
H_2/CH_4	0.96	1.43	1.65	2.00
CO_2/CH_4	1.94	3.17	4.04	4.58
CO_2/N_2	5.10	7.91	10.2	11.1
$\text{C}_2\text{H}_4/\text{C}_2\text{H}_6$	0.88	—	1.02	1.05
$\text{C}_3\text{H}_6/\text{C}_3\text{H}_8$	1.66	—	2.15	2.34

^a $\times 10^{-7}$ [cm^3 (STP) $\text{cm}/\text{cm}^2 \text{ sec cmHg}$].

Figures 6, 7, and 8 show the relationship between bromine content and permeability, diffusion, and solubility coefficients for oxygen in the Br-PMSP membranes at 30°C, respectively. Since most diffusion coefficients were too fast, over 10^{-5} (cm^2/s), membranes of about 450 μm thickness were used to do a more accurate measurement of the time lag. It is clear that the decrease in the permeability coef-

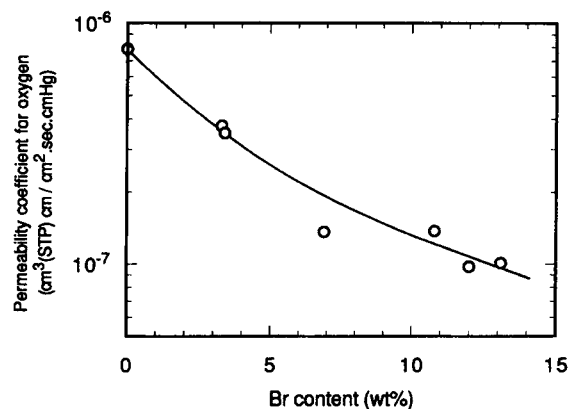


Figure 6 Relationship between bromine content and permeability coefficient for oxygen in the brominated PMSP membranes at 30°C.

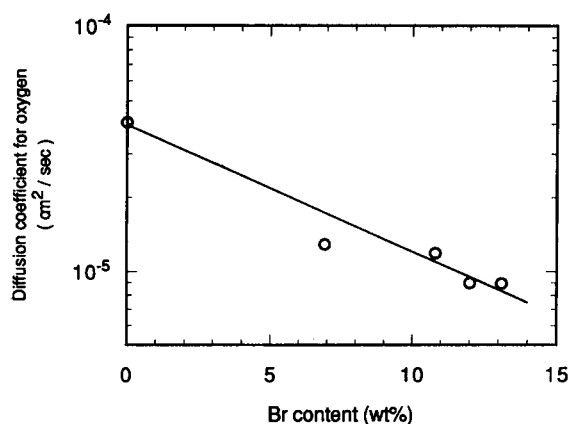


Figure 7 Relationship between bromine content and diffusion coefficient for oxygen in the brominated PMSP membranes at 30°C.

efficient depends on the decrease in the diffusion coefficient. This means that the bromine atoms that reacted with the PMSP could act as inhibitors of the diffusion for penetrants into the membrane.

The d spacing in a polymer means average intersegmental distance. Therefore, this value is often presumed to be sensitive to the degree of polymer chain's packing, i.e., higher d spacings correspond to less closely packed polymer chains and lower d spacings correspond to more densely packed chains. The d spacing is calculated from Bragg's relation:

$$\lambda = 2d \sin \theta \quad (8)$$

where λ is the wavelength of the X-ray radiation (CuK α wavelength = 1.54 Å) and θ is the location of the center of the broad intense peak in the X-ray pattern. Figure 9 shows the X-ray spectra of the

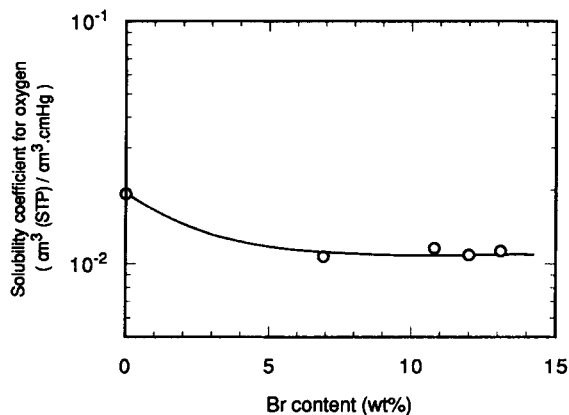


Figure 8 Relationship between bromine content and solubility coefficient for oxygen in the brominated PMSP membranes at 30°C.

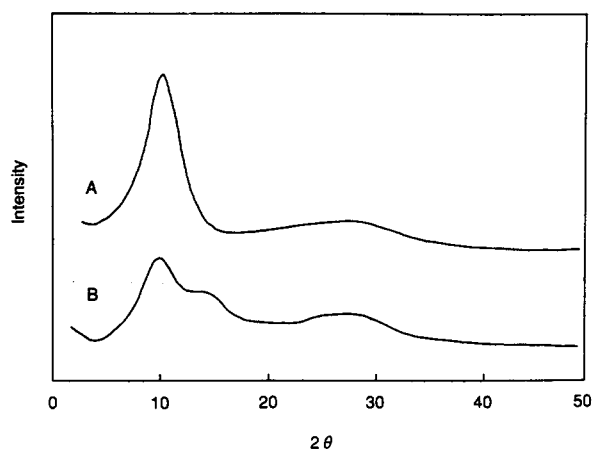


Figure 9 X-ray spectra of the (a) PMSP and (b) brominated PMSP (Br: 6.9 wt %) membranes.

PMSP and Br-PMSP (Br: 6.9 wt %) membranes. The PMSP membrane had an amorphous peak at 10°. The d spacing is then 8.8 Å. This value is very large compared to other glassy polymers.²² The Br-PMSP also had a peak at the same point. However, the peak intensity was smaller than that for the PMSP, and there was a shoulder peak on the high degree side. This result means that the reacted bromine atoms gradually filled the free volume.

Temperature Dependence of Gas Permeability

A distinct change in slope occurs at the T_g in the Arrhenius plot of permeability coefficient in polymeric membranes.²⁵⁻²⁷ Figure 10 shows the temperature dependence of the permeability coefficient for oxygen in the PMSP and Br-PMSP membranes.

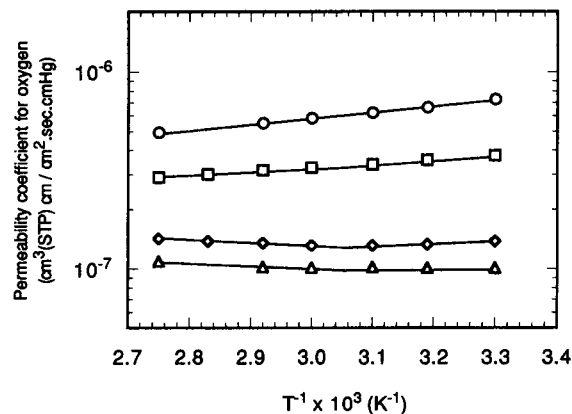


Figure 10 Temperature dependence of permeability coefficients for oxygen in (○) the PMSP membrane and the brominated PMSP membranes containing (□) 3.3, (◇) 10.8, and (△) 13.1 wt % bromine.

There is no transition point in the PMSP, but transition points were observed between 50 and 60°C, i.e., between 3.1×10^{-3} and 3.0×10^{-3} (K^{-1}) in all Br-PMSP. This result is similar to the behavior across the T_g . The E_p of the PMSP membrane had a negative value. In a polymer-gas system, most nonporous polymeric membranes have $E_p > 0$ with $E_D > 0$ and $\Delta H_s < 0$. A PMSP membrane is nonporous, i.e., $E_D > 0$, but it has $E_p < 0$. The negative E_p value came from the large negative value of ΔH_s .^{6,9} The E_p above the transition temperature for all Br-PMSP membranes was larger than that below the point. Since the E_p of most membranes has a negative value, the E_p above the transition point of all Br-PMSP membranes containing over 10 wt % bromine had a positive value. It was assumed that a new local domain, which had a new T_g , was produced by the bromination because the transition temperature clearly appeared in the Br-PMSP with only 3 wt % bromine content.

Figures 11, 12, and 13 show the temperature dependence of permeability, diffusion, and solubility coefficients for various gases in the Br-PMSP (Br: 10.8 wt %) membrane between 30 and 90°C, respectively. The transition points were also observed for all measured gases between 50 and 60°C in the Arrhenius plots of permeability and diffusion coefficients. However, the relation between solubility coefficient and temperature are straight lines. This result also indicates that the permeability of the Br-PMSP membrane depends on diffusibility. The E_p for H_2 , N_2 , O_2 , and CH_4 above the transition temperature had a positive value. In the case of H_2 , the E_p below the transition temperature also showed a positive value.

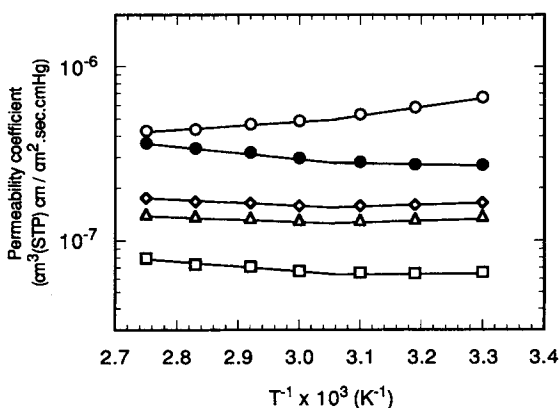


Figure 11 Temperature dependence of permeability coefficient for (○) carbon dioxide, (●) hydrogen, (◇) methane, (△) oxygen, and (□) nitrogen in the brominated PMSP (Br: 10.8 wt %) membrane.

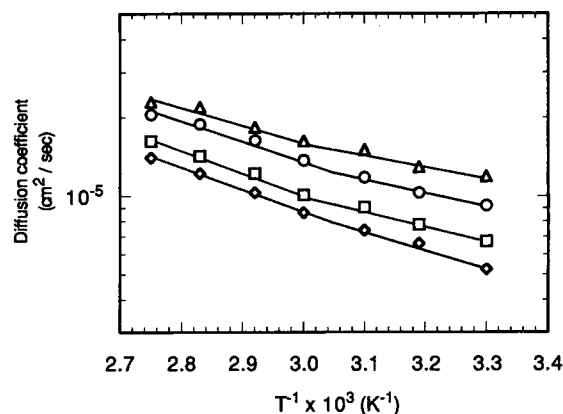


Figure 12 Temperature dependence of diffusion coefficient for (○) carbon dioxide, (◇) methane, (△) oxygen, and (□) nitrogen, in the brominated PMSP (Br: 10.8 wt %) membrane.

Figure 14 shows the relationship between bromine content and activation energies for permeation and diffusion for oxygen in the Br-PMSP membrane. The energies of the Br-PMSP membranes were higher than those of the PMSP membrane. The energy for permeation above the transition temperature had a positive value for bromine contents over 10 wt %. With increasing bromine content, the difference values, i.e., E_p (above transition temperature) $- E_p$ (below transition temperature), increased once, and then decreased. This suggests that, first, flexibility increased due to bromination, and then, the bromine atoms reacted with the PMSP, possibly acting as inhibitors of flexibility in the chains.

Figures 15, 16, and 17 show the temperature de-

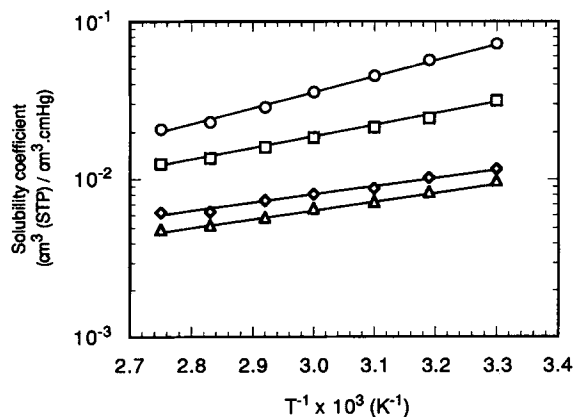


Figure 13 Temperature dependence of solubility coefficient for (○) carbon dioxide, (□) methane, (◇) oxygen, and (△) nitrogen in the brominated PMSP (Br: 10.8 wt %) membrane.

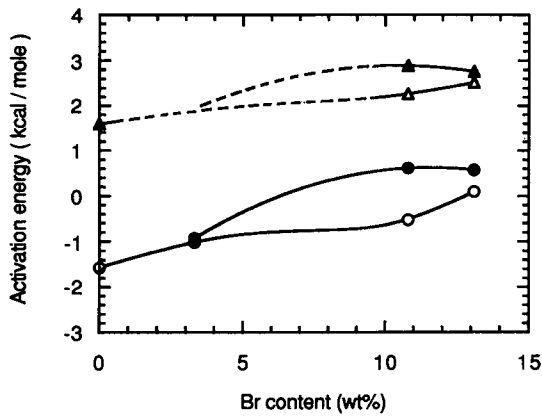


Figure 14 Relationship between bromine content and activation energies for [(○) 30–50°C, (●) 60–90°C] permeation and [(△) 30–50°C, (▲) 60–90°C] diffusion of oxygen in the brominated PMSP membranes.

pendence of ideal separation factors for H₂/N₂, O₂/N₂, and CO₂/N₂ in the PMSP and Br-PMSP membranes, respectively. Most polymeric membranes show a decrease in the ideal separation factors for industrially important gas pairs with increasing measurement temperature. In the case of O₂/N₂ and CO₂/N₂, the same behavior was observed, but the factor for H₂/N₂ increased with increasing temperature. This means that, for example, as shown in Figure 12, the permeability coefficient for H₂ changed from that for N₂ with increasing temperature, however, the coefficients for O₂ and CO₂ approached it. The factors for H₂/N₂ and O₂/N₂ showed linearity in the Arrhenius plots and the transition points were not observed. On the other hand, in the case of the factor for CO₂/N₂, there was

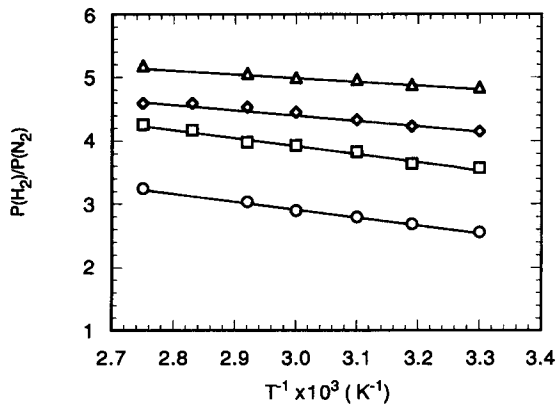


Figure 15 Temperature dependence of ideal separation factors for hydrogen/nitrogen in (○) the PMSP membrane and the brominated PMSP membranes containing (□) 3.3, (◇) 10.8, and (△) 13.1 wt % bromine.

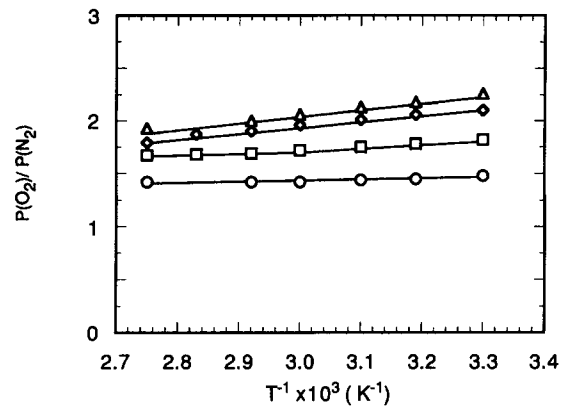


Figure 16 Temperature dependence of ideal separation factors for oxygen/nitrogen in (○) the PMSP membrane and the brominated PMSP membranes containing (□) 3.3, (◇) 10.8, and (△) 13.1 wt % bromine.

a transition point between 50 and 60°C, which is the same temperature region that appeared for the permeation measurement. It was assumed that the transition points might exist in the case of H₂/N₂ and O₂/N₂, but they were apparently hidden because these values were smaller than that for CO₂/N₂.

Durability of Brominated PMSP

The Br-PMSP membrane, itself, had durability that was unexpected. The gas permeation durability in the Br-PMSP membrane is shown in Figure 18. The bromine content in the Br-PMSP was 2.6 wt % and a thin membrane was used. The hysteretic condition was that the membranes were stored under vacuum (10⁻² mm Hg) at 30°C. This temperature is below

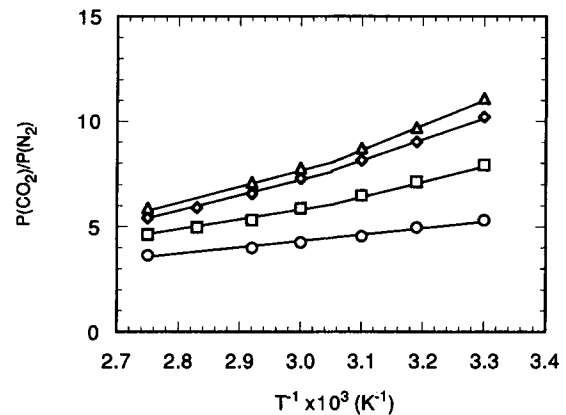


Figure 17 Temperature dependence of ideal separation factors for carbon dioxide/nitrogen in (○) the PMSP membrane and the brominated PMSP membranes containing (□) 3.3, (◇) 10.8, and (△) 13.1 wt % bromine.

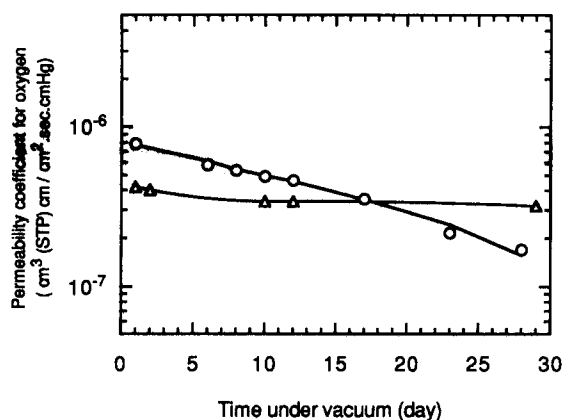


Figure 18 Durability of permeability coefficients for oxygen in the (Δ) brominated PMSP (Br: 2.6 wt %) membrane compared with (\circ) the PMSP membrane (from Ref. 35) at 30°C. Thickness: PMSP; 61 μm , Br-PMSP; 59 μm . Condition: kept under vacuum at 30°C.

the transition temperature as shown in Figure 12. The permeability of the PMSP decreased rapidly, however, that of Br-PMSP was stable. The hysteresis of the PMSP membrane results in a significant physical aging from a quasi-stable to a stable state in comparison with the cases of other polymeric membranes.^{3,4,22} This result suggests that the bromination protected the sites from physical aging. After annealing the membranes above the transition temperature, a slight decrease in permeability was observed in the Br-PMSP membrane. However, the permeability was more stable than that of the PMSP membrane.

CONCLUSIONS

The brominated poly(1-trimethylsilyl-1-propyne) membranes were prepared using the membrane reaction method. However, the bromination of the PMSP membrane occurred not only on the surface but also in the bulk. This reason was that the reaction with bromine and the PMSP was the rate-determining step in comparison to the diffusion of bromine atoms in the membrane.

The bromine mainly reacted with the carbon-carbon double bonds in the backbone chain and carbon-carbon single bonds were produced. A new endothermic transition appeared between 50 and 80°C in the DSC curves of all brominated membranes in spite of the bromine content. In the Arrhenius plots of the permeability, the transition point was observed near the endothermic temperature in all Br-

PMSP membranes. The origin of these transitions would be assigned to the movement change (rotation) in the produced carbon-carbon single bonds. This suggests that a new local domain, which was composed of the produced carbon-carbon single bonds and their neighborhood, was produced and had a new glass transition temperature.

REFERENCES

1. T. Masuda, E. Isobe, T. Higashimura, and K. Takada, *J. Am. Chem. Soc.*, **105**, 7473 (1983).
2. K. Takada, K. Matsuya, T. Masuda, and T. Higashimura, *J. Appl. Polym. Sci.*, **30**, 1605 (1985).
3. H. Shimomura, K. Nakanishi, H. Odani, M. Kurata, T. Masuda, and T. Higashimura, *Kobunshi Ronbunshu*, **43**, 747 (1986).
4. Y. Ichiraku, S. A. Stern, and T. Nakagawa, *J. Memb. Sci.*, **34**, 5 (1987).
5. J. F. Kunzler and V. Percec, *Polym. Bull.*, **18**, 303 (1987).
6. T. Nakagawa, T. Saito, S. Asakawa, and Y. Saito, *Gas Separation and Purification*, **2**, 3 (1988).
7. M. Langson, M. Andard, and E. J. Karwachi, *Gas Separation and Purification*, **2**, 162 (1988).
8. T. N. Bowmer and G. L. Baker, *Polym. Prepr. ACS*, **27** (2), 218 (1986).
9. T. Masuda, Y. Iguchi, B-Z. Tang, and T. Higashimura, *Polymer*, **29**, 2041 (1988).
10. S. Asakawa, Y. Saito, K. Waragai, and T. Nakagawa, *Gas Separation and Purification*, **3**, 117 (1989).
11. K. Takada, Z. Ryugo, and H. Matsuya, *Kobunshi Ronbunshu*, **46**, 1 (1989).
12. K. Takada, Z. Ryugo, and H. Matsuya, *Kobunshi Ronbunshu*, **46**, 7 (1989).
13. K. Takada, Z. Ryugo, and H. Matsuya, *Kobunshi Ronbunshu*, **46**, 63 (1989).
14. T. Nakagawa, H. Nakano, K. Enomoto, and A. Higuchi, *AIChE Symposium Series*, No. 272, **85**, 1 (1989).
15. L. C. Witchey-Lakshmanan, H. B. Hopfenberg, and R. T. Chern, *J. Memb. Sci.*, **48**, 321 (1990).
16. Y. Nagase, S. Mori, K. Ishihara, K. Matsui, and M. Uchikura, *J. Polym. Sci., Polym. Phys. Ed.*, **29**, 171 (1991).
17. N. A. Platé, A. K. Bokarev, N. E. Kaliuzhnyi, E. G. Litvinova, V. S. Khotimskii, V. V. Volkov, and Y. P. Yampol'skii, *J. Memb. Sci.*, **60**, 13 (1991).
18. X. Lin, J. Xiao, Y. Yu, J. Chen, G. Zheng, and J. Xu, *J. Appl. Polym. Sci.*, **48**, 231 (1992).
19. Y. P. Yampol'skii, V. P. Shantorovich, F. P. Chernyakovskii, A. I. Kornilov, and N. A. Platé, *J. Appl. Polym. Sci.*, **47**, 85 (1993).
20. K. K. Hsu, S. Nataraj, R. M. Thorogood, and P. S. Puri, *J. Memb. Sci.*, **79**, 1 (1993).

21. G. Chen, H. J. Griesser, and A. W. H. Mau, *J. Memb. Sci.*, **82**, 99 (1993).
22. T. Nakagawa, S. Fujisaki, H. Nakano, and A. Higuchi, *J. Memb. Sci.*, to appear.
23. T. Masuda, E. Isobe, and T. Higashimura, *Macromolecules*, **18**, 841 (1985).
24. T. Masuda and T. Higashimura, *Adv. Polym. Sci.*, **81**, 122 (1987).
25. T. Nakagawa, H. B. Hopfenberg, and V. Stannett, *J. Appl. Polym. Sci.*, **15**, 231 (1971).
26. V. Stannett, *Diffusion in Polymers*, Academic Press, London, 1968, p. 41.
27. T. Nakagawa, *Membrane Science and Technology*, Dekker, New York, 1992, p. 239.
28. W. A. Lee and R. A. Rutherford, *Polymer Handbook*, 2nd ed., Wiley, New York, 1975, III-139.
- 29.(a) H. Burrell, *Polymer Handbook*, 2nd ed., Wiley, New York, 1975, IV-339. (b) R. F. Fedors, *Polym. Eng. Sci.*, **14**, 147 (1974).
30. T. Nakagawa and S. Yamada, *J. Appl. Polym. Sci.*, **16**, 1997 (1972).
31. G. H. Schmid and B. Toyonaga, *J. Org. Chem.*, **49**, 761 (1984).
32. M-F. Ruasse and B-L. Zhang, *J. Org. Chem.*, **49**, 3207 (1984).
33. M-F. Ruasse and E. Lefebvre, *J. Org. Chem.*, **49**, 3210 (1984).
34. G. Cerichelli, C. Grande, L. Luchetti, and G. Mancini, *J. Org. Chem.*, **56**, 3025 (1991).
35. K. Nagai, A. Higuchi, and T. Nakagawa, submitted for publication.

Received December 27, 1993

Accepted May 10, 1994